Machine-Checked Sign-Vector Kernel and Exact-Rational Certificates for Flag Targets, Quasipolyhedral Non-Attainment, Frame Slices, and Acyclic Chamber DAGs

Lluis Eriksson*

November 25, 2026

Abstract

Brennan Dury (`arXiv:2611.32976`, November 24, 2026) constructed objective-driven acyclic digraphs on chambers of locally finite affine hyperplane arrangements: from each objective-bounded chamber c, a codimension-r flag at its optimal face F yields $2^r - 1$ outgoing targets via a sign-flip rule, and both Euclidean and Frame strategies force escape to strictly higher optimal values in bounded steps. We deliver an explicitly scoped, zero-floating-point verification stack pairing two complementary layers. First, an 18-theorem zero-dependency Lean 4.35.0 kernel (`HyperplaneTraversal.lean`; 0 `sorry`, 0 warnings, 0 `Classical.choice`; 5 zero-axiom, 1 `[propext]`, 12 `[propext, Quot.sound]`) proves single-coordinate sign-closure poset axioms, combinatorial sign-flip counting/distinctness/containment identities, cleared integer/inductive laws of Section 2 Figure 2's quasipolyhedral non-attainment counterexample ($\ell_n(x) = 2^{-(n+1)}(x - n - 2)$), and scalar algebraic projections of Lemma 4, Lemma 15, Lemma 17, Proposition 3 (`lexLt3`), and Theorem 3. Second, `ARRANGEMENT-TRAVERSAL-CERT-1.0` performs full multi-dimensional exact-$\mathbb{Q}$ verification of codimension ranks, Figure 2 truncations, full-rank Frame slices, and strict-complementarity KKT chamber DAGs across 16 canonical certificates (0.110–1.003 ms)—including a fully specified 8-chamber 4-line central fan DAG ($L = 3$)—while rejecting 66/66 live adversarial forgeries.

1 Introduction and Scope Calibration

Classical chamber-traversal constructions on real hyperplane arrangements—such as Edelman's walk [4] and Salvetti–Settepanella polar paths [5]—navigate toward a fixed base chamber. Brennan Dury [3] introduced objective-driven acyclic chamber digraphs on locally finite affine hyperplane arrangements $\mathcal{P}$ with a nonconstant affine objective ω, built on four algebraic and geometric mechanisms:

1. *Sign-vector face calculus & Theorem 2 targets:* Faces are nonempty relatively open fibres of $x \mapsto \operatorname{sign}_{\mathcal{P}}(x) \in \{-1, 0, +1\}^{\mathcal{P}}$, ordered by closure containment $E \subseteq \overline{F} \iff \forall q,\ \operatorname{sign}_E(q) \in \{0, \operatorname{sign}_F(q)\}$ (Proposition 1). A codimension-r flag of faces $F = F_r, F_{r-1}, \ldots, F_0 = c$ with $F_i \subseteq \overline{F_{i-1}}$ and $\operatorname{codim}(F_i) = i$ partitions the vanishing forms $Q(F, \mathcal{P}) = Q_1 \sqcup \cdots \sqcup Q_r$ into nonempty layers $Q_i := Q(F_i, \mathcal{P}) \setminus Q(F_{i-1}, \mathcal{P})$; writing $\ell(q) \in \{1, \ldots, r\}$ for the unique layer index with $q \in Q_{\ell(q)}$, every $\alpha \in \{\pm 1\}^r \setminus \{1^r\}$ defines one of $2^r - 1$ distinct outgoing target chambers $b_{\mathrm{FL}}(\alpha)$ [1] via
$$\operatorname{sign}_{b_{\mathrm{FL}}(\alpha)}(q) = \begin{cases} \alpha_{\ell(q)} \operatorname{sign}_c(q), & q \in Q(F, \mathcal{P}), \\ \operatorname{sign}_c(q), & q \notin Q(F, \mathcal{P}). \end{cases} \tag{1}$$
2. *Figure 2 quasipolyhedral non-attainment (Section 2):* While every bounded-above affine objective on a closed face of a locally finite arrangement attains its supremum (Theorem 1), $C = \{(x, y) : y \le \ell_n(x)\ \forall n \ge 0\}$ with $\ell_n(x) = 2^{-(n+1)}(x - n - 2)$ has $y < 0$ everywhere yet $\omega(p_n) = -2^{-n} \to 0$; every line H_n hits $\{0\} \times [-1, 0]$ at $y_n = -(n + 2)2^{-(n+1)}$, violating local finiteness.
3. *Frame slice recursion & strict potential (Section 6, Lemma 17, Proposition 3):* Normalizing tangent-cone generators onto $P_\eta(c, G) = R_G(c) \cap \{\eta = -1\}$ via $v_H = -\xi_H / \eta(\xi_H)$ and uniquely maximizing an admissible frame covector φ yields strictly negative next covector values $\eta^+(q - p) = \varphi(q) - \varphi(p) < 0$, strictly increasing the $(r + 1)$-component lexicographic potential $P^*_{\mathcal{F}}(c) = (\lambda(c, \omega), \dim F(c, \omega), S^{\mathcal{F}}_r(c), \ldots, S^{\mathcal{F}}_2(c))$.
4. *Acyclicity & uniform escape length L (Theorem 3 & Theorem 5):* Because $G_{\mathcal{F}}$ is acyclic on finite level sets, every directed walk of length $L = L_{\max} + 1$ escapes strictly above its starting optimal value $\lambda(c_0, \omega)$.

Honest Two-Layer Scope Calibration. We distinguish strictly between what is proved universally in Lean 4 vs. verified in full dimension on finite rational witnesses vs. left in [3]:

1. **Lean 4 kernel (§2, Table 1):** 18 zero-dependency constructive theorems in `HyperplaneTraversal.lean` (Lean 4.35.0 [2]; 0 `sorry`, 0 warnings, 0 `Classical.choice`). Table 1 prints every exact theorem type, hypothesis, and axiom footprint verbatim.

*Independent researcher; manuscript prepared with transparent AI assistance via Google Antigravity. Source code (MIT), Lean 4 proofs (MIT), and manuscript/figures (CC-BY-4.0): https://github.com/lluiseriksson/hyperplane-arrangement-traversal-certificates.

2. **Exact-$\mathbb{Q}$ multi-dimensional verifier (§3, Table 2):** `ARRANGEMENT-TRAVERSAL-CERT-1.0` performs full vector-space Gaussian rank checks, exact Figure 2 feasibility, full-rank Frame slices, and strict-complementarity KKT chamber DAG certification with zero floats.
3. **Explicit non-claims:** Our Lean 4 kernel does *not* formalize general vector-space hyperplane arrangements, polyhedral faces, LP duality, multi-dimensional chamber DAGs, Theorem 1 compactness, or Lemma 18 Zariski-open admissibility; Theorems 1–8 and 13–18 formalize their exact single-coordinate sign calculus, counting identities, and cleared scalar/3-tuple algebraic projections, while multi-dimensional geometry is audited by `ARRANGEMENT-TRAVERSAL-CERT-1.0`.

2 Zero-Dependency Lean 4 Kernel

`lean/HyperplaneTraversal.lean` compiles standalone under Lean 4.35.0 with zero external dependencies and is audited by `AuditAxioms.lean` with 0 warnings, 0 `sorry`, 0 `Classical.choice`, and 0 `Lean.ofReduceBool`: 5 zero-axiom (`none`: #1–3, #5, #7), 1 `[propext]` (#6), and 12 `[propext, Quot.sound]`.

Proposition 1 (Constructive Scope of `HyperplaneTraversal.lean`)**.** All 18 statements in Table 1 hold constructively without external libraries or `Classical.choice`. In particular, Theorem 11 inductively proves $0 < n + 2 \le 2^{n+1}$ for all $n \in \mathbb{N}$ (showing every line H_n of Figure 2 meets $\{0\} \times [-1, 0]$), Theorem 14 proves strict partial-order acyclicity of `lexLt3`, Theorem 15 proves Lemma 17's negative next covector $\varphi_q - \varphi_p < 0 < \varphi_p - \varphi_q$, and Theorem 16 proves $\eta_\xi = (-1)D < 0$ under the explicit hypothesis $0 < D$.

3 Exact-$\mathbb{Q}$ Verifier Architecture

The pure-stdlib zero-float verifier `src/arrangement_certifier.py` (`ARRANGEMENT-TRAVERSAL-CERT-1.0`) enforces strict JSON typing, canonical reduced rationals, and uniform 2048-bit / 1024-char / 128-char ID bounds across four modes:

1. **Mode 1 (Theorem 2 Flag Sign Targets):** Evaluates interior witness points along $F_0 = c, F_1, \ldots, F_r = F$ with $F_i \subseteq \overline{F_{i-1}}$, verifies exact Gaussian codimension rank $\operatorname{rank}(Q(F_i, \mathcal{P})) = i$ at every level and exact layer partition $Q_1 \sqcup \cdots \sqcup Q_r$, and certifies that all $2^r - 1$ target witnesses realize (1), are pairwise distinct, and contain F in their closures.
2. **Mode 2 (Section 2 Figure 2 Counterexample):** Independently verifies exact interpolation $p_k = (k, -2^{-k}) \in H_k \cap H_{k-1}$, all $(N+1)^2$ halfplane inequalities $y(p_k) \le \ell_n(x(p_k))$, compact-segment intercepts $y_0(H_n) = -(n+2)2^{-(n+1)} \in [-1, 0)$, and exact gap $0 - \omega(p_N) = 2^{-N}$.

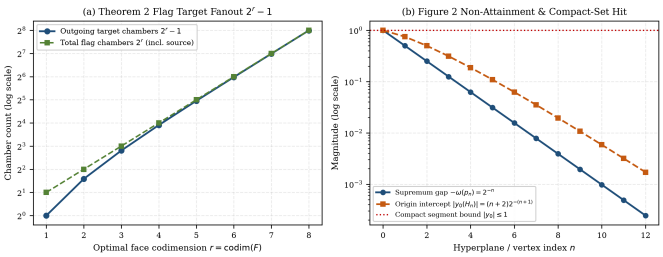

Figure 1: (a) Exact Theorem 2 outgoing target fanout $2^r - 1$ vs. total flag chambers 2^r across codimensions $r = 1 \ldots 8$. (b) Section 2 Figure 2 exact supremum gap $-\omega(p_n) = 2^{-n}$ and origin intercept $|y_0(H_n)| = (n+2)2^{-(n+1)} \le 1$ across $n = 0 \ldots 12$.

3. **Mode 3 (Section 6 Frame Slice & Potential):** Enforces full-rank tangent cones ($\operatorname{rank} = d$), pairwise distinct slice vertices $v_k = -\xi_k/\eta(\xi_k) \in \{\eta = -1\}$ with distinct source/target slices, valid face dimensions $0 \le \dim F < d$, unique admissibility of $\arg\max \varphi(v_k)$, Lemma 17 next-covector negativity $\eta^+(q - p) = \varphi(q) - \varphi(p) < 0$ on $\ker \eta$, and strict increase $P^*(c) <_{\text{lex}} P^*(b)$.
4. **Mode 4 (Acyclic Chamber DAG & Escape L):** On every objective-bounded chamber c, enforces non-negativity $y_k \ge 0$, strict complementarity ($y_k > 0 \iff q_k(x^*) = 0$, $y_k = 0 \iff q_k(x^*) \ne 0$), and LP dual stationarity $c_\omega + \sum_k y_k \sigma_k a_k = 0$ certifying $x^* \in \operatorname{relint}(F(c))$ and $\dim F(c) = d - \operatorname{rank}(Q(F(c), \mathcal{P}))$; on every objective-unbounded chamber, verifies a positive recession ray and canonical zero/empty fields. It then checks that every objective-bounded chamber's outgoing edges match all $2^r - 1$ Theorem 2 targets of its flag layers with $F(c) \subseteq \bar{b}$, checks strict increase of the certified 3-tuple potential proxy $(\lambda, \dim F, S)$ (exact for $r \le 2$, and sufficient on our $r = 3$ octant where all targets jump to $\lambda = \infty$; Dury's general $P^*_{\mathcal{F}}$ has $r + 1$ components for $r \ge 3$), certifies Kahn DAG acyclicity, and computes $L = L_{\max} + 1$.

4 Empirical Atlas, Explicit 4-Line Fan, and Red-Team Audit

Running `scripts/run_all_experiments.py` produces all 16 canonical certificates (Table 2) and four exact-$\mathbb{Q}$ datasets, audited end-to-end by `scripts/verify_all.py` with SHA-256 verification across all 41 tracked files.

Explicit Verification of the 8-Chamber 4-Line Central Fan DAG (Fig. 2(a)). Certificate #15 uses the four central lines $H_0 : x_2 = 0$, $H_1 : x_1 = 0$, $H_2 : x_1 - x_2 = 0$, $H_3 : x_1 + x_2 = 0$ and objective $\omega(x) = x_2$. In the lower half-plane ($x_2 < 0$), the four objective-bounded sectors are, from left to right:

- c_{LL} at $(-2, -1)$, signs $(-, -, -, -)$: adjacent to H_0, so $F = \{x_2 = 0, x_1 \le 0\}$ ($\dim 1$), $x^* = (-1, 0)$, $y = (1, 0, 0, 0)$, layer $[[0]]$, unique target $c_{\text{UL}} = (+, -, -, -)$ at $(-2, 1)$.

Table 1: Complete inventory of all 18 Lean 4.35.0 theorems in `lean/HyperplaneTraversal.lean` with exact quantified statements, hypotheses, and audited axiom footprints (0 `sorry`, 0 warnings, 0 `Classical.choice`; `P,Q` abbreviates `[propext, Quot.sound]`).

#	Lean 4 Theorem Identifier	Exact Machine-Checked Statement & Hypotheses	Axioms
1	`sign_closure_reflexive`	$\forall s \in \texttt{Sign},\ \texttt{signLe}\ s\ s$ (where $\texttt{signLe}\ a\ b :\Longleftrightarrow\ a = 0 \vee a = b$).	none
2	`sign_closure_transitive`	$\forall a, b, c \in \texttt{Sign},\ \texttt{signLe}\ a\ b \to \texttt{signLe}\ b\ c \to \texttt{signLe}\ a\ c$.	none
3	`sign_closure_antisymmetric`	$\forall a, b \in \texttt{Sign},\ \texttt{signLe}\ a\ b \to \texttt{signLe}\ b\ a \to a = b$.	none
4	`theorem2_target_count_formula`	$\forall r \in \mathbb{N},\ 1 \le r \to 1 + (2^r - 1) = 2^r \wedge 1 \le 2^r - 1$.	P,Q
5	`theorem2_sign_identity_at_ones`	$\forall s \in \texttt{Sign},\ \texttt{flipSign true}\ s = s$.	none
6	`theorem2_distinct_targets_opposite_sign`	$\forall a, b \in \texttt{Bool},\ s \in \texttt{Sign},\ s \neq 0 \to a \neq b \to \texttt{flipSign}\ a\ s \neq \texttt{flipSign}\ b\ s$.	propext
7	`theorem2_base_containment_preserved`	$\forall \alpha \in \texttt{Bool},\ s \in \texttt{Sign},\ \texttt{signLe}\ 0\ (\texttt{flipSign}\ \alpha\ s)$.	none
8	`lemma4_weak_objective_increase`	$\forall \lambda_c, \lambda_b, x^* \in \mathbb{Z},\ \lambda_c = x^* \to x^* \le \lambda_b \to \lambda_c \le \lambda_b$ (scalar projection).	P,Q
9	`fig2_line_passes_through_pn_and_pn1`	$\forall n \in \mathbb{Z},\ (n - n - 2 = -2) \wedge ((n+1) - n - 2 = -1)$ (cleared $\ell_n(p_n), \ell_n(p_{n+1})$).	P,Q
10	`fig2_line_envelope_domination`	$\forall n, x \in \mathbb{Z},\ (x - (n+1) - 2) - 2(x - n - 2) = (n+1) - x$ (cleared envelope step).	P,Q
11	`fig2_origin_intercept_in_compact_unit_segment`	$\forall n \in \mathbb{N},\ 0 < n + 2 \wedge n + 2 \le 2^{n+1}$ (inductive proof $y_0(H_n) \in [-1, 0)$).	P,Q
12	`fig2_strict_negativity_on_C`	$\forall x, n \in \mathbb{Z},\ x + 1 \le n \to x - n - 2 \le -3 \wedge x - n - 2 < 0$.	P,Q
13	`opposite_ray_negativity_impossible`	$\forall u \in \mathbb{Z},\ u < 0 \to -u < 0 \to \bot$ (scalar opposite-ray contradiction).	P,Q
14	`lex_potential_strict_increase_trans`	$\forall a, b, c \in \mathbb{Z}^3,\ \texttt{lexLt3}\ a\ b \to \texttt{lexLt3}\ b\ c \to \texttt{lexLt3}\ a\ c \wedge \neg\texttt{lexLt3}\ a\ a$.	P,Q
15	`lemma17_slice_denominator_positive`	$\forall \varphi_p, \varphi_q \in \mathbb{Z},\ \varphi_q < \varphi_p \to \varphi_q - \varphi_p < 0 \wedge 0 < \varphi_p - \varphi_q$.	P,Q
16	`slice_vertex_normalization_identity`	$\forall \eta_\xi, D \in \mathbb{Z},\ 0 < D \to \eta_\xi = -D \to \eta_\xi = (-1) \cdot D \wedge \eta_\xi < 0$.	P,Q
17	`dag_escape_length_bound`	$\forall r_0, t, K \in \mathbb{N},\ r_0 + t < K \to t < K$ (scalar rank-escape bound).	P,Q
18	`euclidean_inner_product_opposite_unit_neg`	$\forall u_c, u_b \in \mathbb{Z},\ u_c < 0 \to -u_c \le u_b \to u_b < 0 \to \bot$ (scalar Lem. 15 projection).	P,Q

Table 2: Complete 16-certificate `ARRANGEMENT-TRAVERSAL-CERT-1.0` atlas with explicit dimensions, parameters, exact certified witness invariants, and median zero-float replay latencies (all 16 verified; 66/66 live adversarial attacks rejected).

#	Certificate ID	Mode	Explicit Certified Parameters	ms
1	`m1_flag_2d_axes_fig4_panel1`	M1	d=2, r=2 (Dury Fig. 4a: $x_1, x_2, x_1{+}x_2{=}0$): layers [[1], [0, 2]], 3 distinct targets.	0.147
2	`m1_flag_2d_axes_fig4_panel2`	M1	d=2, r=2 (Dury Fig. 4b: $x_1, x_2, x_1{+}x_2{=}0$): layers [[0], [1, 2]], 3 distinct targets.	0.148
3	`m1_flag_3d_coupled_codim3`	M1	d=3, r=3 (5 coupled planes): layers [[2], [1, 4], [0, 3]], exact ranks 0, 1, 2, 3, 7 targets.	0.344
4	`m1_flag_4d_affine_codim4_15targets`	M1	d=4, r=4 (7 planes, 1 non-central): layers [[3], [2, 5], [1], [0, 4]], 15 distinct targets.	1.003
5	`m2_fig2_counterexample_N4`	M2	Sec. 2 Fig. 2 truncation N=4: 25 halfplane checks, $y_0 \in [-1, 0)$, gap = 1/16.	0.137
6	`m2_fig2_counterexample_N8`	M2	Sec. 2 Fig. 2 truncation N=8: 81 halfplane checks, $y_0 \in [-1, 0)$, gap = 1/256.	0.256
7	`m2_fig2_counterexample_N12`	M2	Sec. 2 Fig. 2 truncation N=12: 169 halfplane checks, $y_0 \in [-1, 0)$, gap = 1/4096.	0.506
8	`m2_fig2_counterexample_N16`	M2	Sec. 2 Fig. 2 truncation N=16: 289 halfplane checks, $y_0 \in [-1, 0)$, gap = 1/65536.	0.860
9	`m3_frame_2d_same_face_lex_step`	M3	d=2, full-rank cones: λ=0, $\dim F$=0, $S^{\mathcal{F}} : -1/2 \to 1$, $\eta^+ = -5/2 < 0$.	0.110
10	`m3_frame_3d_simplex_slice_step`	M3	d=3, simplicial cones: λ=5, $\dim F$=0, $S^{\mathcal{F}} : 0 \to 1$, $\eta^+ \in \{-2, -1\}$.	0.168
11	`m3_frame_3d_dim_jump_step`	M3	d=3, full-rank cones: λ=3, $\dim F : 0 \to 1$, $\eta^+ \in \{-5/2, -2\}$.	0.186
12	`m3_frame_4d_objective_jump_step`	M3	d=4, full-rank cones: $\lambda : 2 \to 7/2$, $\dim F$=0, $\eta^+ \in \{-3, -2, -1\}$.	0.265
13	`m4_dag_2d_cross_4chambers`	M4	d=2 cross (x_1, x_2=0), $\omega{=}x_1{+}2x_2$: 1 obj-bounded, 3 unbounded, $L_{\max}$=0, L=1.	0.201
14	`m4_dag_2d_grid_9chambers`	M4	d=2 2×2 grid, $\omega{=}x_1{+}2x_2$: 4 obj-bounded, 5 unbounded, $L_{\max}$=0, L=1.	0.580
15	`m4_dag_2d_degenerate_escape_L3`	M4	d=2 4-line fan ($H_0..H_3$), $\omega{=}x_2$: 4 obj-bounded, 4 unbounded, $L_{\max}$=2, L=3.	0.683
16	`m4_dag_3d_octants_8chambers`	M4	d=3 octants, $\omega{=}x_1{+}2x_2{+}3x_3$: 1 obj-bounded (7 edges), 7 unbounded, L=1.	0.341

- c_{LM} at $(-1, -2)$, signs $(-, -, +, -)$: bounded above by $x_1 \le 0$ and $x_2 \le x_1$, so $F = \{(0, 0)\}$ ($\dim 0$) with strict-complementarity KKT $y = (1/4, 1/4, 1/2, 1/4) \ge 0$ satisfying $(0, 1) + \sum y_k \sigma_k a_k = (0, 0)$. Layers [[1], [0, 2, 3]] flip $\{1\} \mapsto (-, +, +, -) = c_{\mathrm{RM}}$, $\{0, 2, 3\} \mapsto (+, -, -, +) = c_{\mathrm{UML}}$ at $(-1, 2)$, and $\{0, 1, 2, 3\} \mapsto (+, +, -, +) = c_{\mathrm{UMR}}$ at $(1, 2)$.
- c_{RM} at $(1, -2)$, signs $(-, +, +, -)$: bounded above by $x_1 \ge 0$ and $x_2 \le -x_1$, so $F = \{(0, 0)\}$ ($\dim 0$) with $y = (1/4, 1/4, 1/4, 1/2) \ge 0$. Layers [[3], [0, 1, 2]] flip $\{3\} \mapsto (-, +, +, +) = c_{\mathrm{RR}}$, $\{0, 1, 2\} \mapsto (+, -, -, -) = c_{\mathrm{UL}}$, and $\{0, 1, 2, 3\} \mapsto (+, -, -, +) = c_{\mathrm{UML}}$.
- c_{RR} at $(2, -1)$, signs $(-, +, +, +)$: adjacent to H_0, so $F = \{x_2 = 0, x_1 \ge 0\}$ ($\dim 1$), $x^* = (1, 0)$, $y = (1, 0, 0, 0)$, layer [[0]], unique target $c_{\mathrm{UR}} = (+, +, +, +)$ at $(2, 1)$.

Thus $c_{\mathrm{LM}}(\dim 0) \to c_{\mathrm{RM}}(\dim 0) \to c_{\mathrm{RR}}(\dim 1) \to c_{\mathrm{UR}}(\infty)$ is an exact certified walk with $L_{\max} = 2$ and $L = 3$, matching Eq. (1) on every single edge.

Replay Atlas and 66/66 Red-Team Audit (Fig. 3). All 16 canonical certificates replay in 0.110–1.003 ms with zero floats. Our red-team suite (`tests/test_suite.py`) tests 66 live forgery attacks (12 global schema/type/rational + 13 Mode 1 + 12 Mode 2 + 14 Mode 3 + 15 Mode 4—including float/`None`/bool injection, unreduced fractions, codimension rank-jump bypasses, broken flag closures, miss-

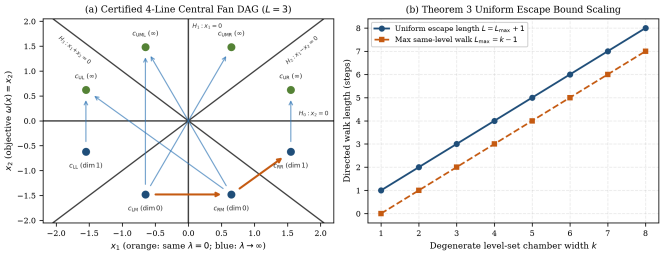

Figure 2: (a) Certified 8-chamber 4-line central fan DAG ($H_0 : x_2{=}0$, $H_1 : x_1{=}0$, $H_2 : x_1{-}x_2{=}0$, $H_3 : x_1{+}x_2{=}0$) under $\omega(x) = x_2$: orange same-level path $c_{\mathrm{LM}} \to c_{\mathrm{RM}} \to c_{\mathrm{RR}}$ ($\lambda = 0$) and blue escape edges ($\lambda \to \infty$), giving $L = 3$. (b) Theorem 3 uniform escape length $L = L_{\max} + 1$ scaling across level-set widths $k = 1 \ldots 8$.

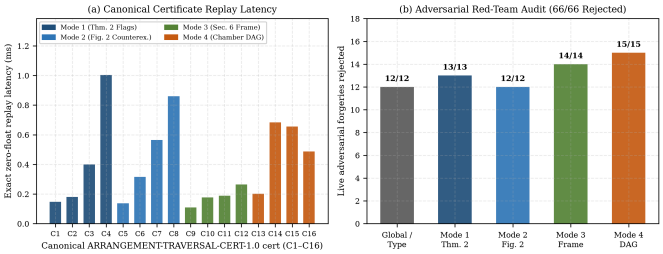

Figure 3: (a) Exact zero-float replay latency across all 16 canonical certificates (0.110–1.003 ms). (b) Live adversarial red-team audit rejecting 66/66 forgeries across five attack classes.

ing Theorem 2 targets, forged Figure 2 vertices/intercepts, rank-deficient cones, negative y_k, boundary-x^* strict-complementarity bypasses, forged $\dim F$, dropped DAG edges, and cycles), achieving **66/66 rejections** with zero bypasses.

5 Conclusion

We delivered an explicitly scoped 18-theorem zero-dependency Lean 4.35.0 kernel (0 `sorry`, 0 warnings, 0 `Classical.choice`, 5 zero-axiom theorems) paired with the exact-$\mathbb{Q}$ multi-dimensional verifier `ARRANGEMENT-TRAVERSAL-CERT-1.0`, 16 explicit canonical certificates (0.110–1.003 ms), full explicit verification of the 8-chamber 4-line central fan DAG ($L = 3$), and 66/66 live adversarial forgery rejections.

References

[1] Marcelo Aguiar and Swapneel Mahajan. *Topics in Hyperplane Arrangements*, volume 226 of *Mathematical Surveys and Monographs*. American Mathematical Society, 2017.

[2] Leonardo de Moura and Sebastian Ullrich. The Lean 4 theorem prover and programming language. In *Automated Deduction – CADE 28*, pages 625–635. Springer, 2021.

[3] Brennan Dury. Traversing hyperplane arrangements with an affine objective. arXiv:2611.32976 [math.CO], 2026.

[4] Paul H. Edelman. A partial order on the regions of $\mathbb{R}^n$ dissected by hyperplanes. *Transactions of the American Mathematical Society*, 283(2):617–631, 1984.

[5] Mario Salvetti and Simona Settepanella. Combinatorial Morse theory and minimality of hyperplane arrangements. *Geometry & Topology*, 11(3):1733–1766, 2007.